

Technical Notes

TECHNICAL NOTES are short manuscripts describing new developments or important results of a preliminary nature. These Notes cannot exceed 6 manuscript pages and 3 figures; a page of text may be substituted for a figure and vice versa. After informal review by the editors, they may be published within a few months of the date of receipt. Style requirements are the same as for regular contributions (see inside back cover).

Flow Structures Formed by Axisymmetric Spinning Bodies

Y. Kohama*

Tohoku University, Sendai, Japan

Introduction

THROUGH the study of flow structures in a three-dimensional boundary layer attached to an axisymmetric rotating body, one might obtain practical understanding of the flight dynamics of such a spinning body. This problem has been one of considerable interest.¹⁻⁷ However, due to its complicated nature, much still needs to be clarified about this problem, particularly with regard to the transition to instability in the boundary layer. This transition to instability is the topic of this Note, in which experimental results are presented.

Experimental Apparatus and Procedure

The experiments were conducted in a small low-turbulence wind tunnel⁸ at Tohoku University. The turbulence intensity at the test section was 0.05-0.15% at the experimental velocity range of 1-14 m/s. The wind tunnel model used was an ogive nose cone whose cross-sectional diagram is shown in Fig. 1. The flow over the nose cone was visualized by applying titanium tetrachloride to the surface of the body in another visualization wind tunnel.⁹ For visualizing a thin boundary layer, this technique is very effective since the smoke is extremely dense and flows only within the boundary layer. However, this method is also rather hazardous because of the presence of poisonous chlorine gas in the smoke. As a consequence, this experiment can be performed only in a controlled environment.

Results

Boundary layers on a spinning ogive nose cone are visualized in Fig. 2. The uniform flow is traveling from right to left. The nose cone is spinning in a counterclockwise direction as viewed from the upstream position. At the most upstream portion of the ogive (the tip), the titanium tetrachloride smoke appears to be smooth. However, as one moves downstream from this smooth laminar region, one observes many spiral streaks. This region of spiral streaks defines the transition region of the boundary layer. This transition region was also observed by Mueller et al.,⁴ who theorized that this particular instability was the result of cross-flow instability. However, when illuminated by a slit strobe light as seen in Fig. 3, these spiral streaks were found to be counterrotating vortices. This phenomena was also observed in the flow around a rotating cone.⁵ It is the

author's opinion that these spiral vortices are a form of dynamic instability induced by the centrifugal force of the flowfield, rather than a cross-flow instability (inflexional instability). The reasoning behind this belief is that, with cross-flow instability, one would expect both corotating vortices¹⁰ and inflexional velocity profiles,¹¹ such as those expected for a rotating disk. However, in the flowfield of the spinning nose cone, only counterrotating vortices were observed with a small component of inflexional velocity (which in this case was induced by the uniform flow component of the centrifugal force, as would be expected in the ogive portion of the body). In the limiting case of the rotating cone in a still fluid, it was found by the author⁹ that counterrotating vortices transform into corotating vortices at approximately the total included angle (2θ , see Fig. 1) of 60 deg. At the total angle of 180 deg, which corresponds to a rotating disk, the flowfield is completely dominated by cross-flow instability (corotating vortices). However, at the total angle of 0 deg, which corresponds to a rotating cylinder, the flowfield is completely dominated by centrifugal instability (counterrotating vortices). Based on these limiting cases, we see that corotating vortices and counterrotating vortices are complementary instabilities whose relative strengths are equal only at approximately a total angle of 60 deg. When uniform flow was applied, it was found that this transition angle became smaller (roughly between 30 and 60 deg) rather than the 60 deg observed for still fluid.

The boundary-layer velocity profile of a cone of total angle 30 deg was also measured.¹² There appears to be no typical boundary-layer velocity profile that contains an inflexion point. Although the shape of the bodies may be different, it seems that the velocity profiles do not differ by very much. Therefore, it is expected that the same kind of velocity profile is observed on a cone will also be found on an ogive nose cone. Based on these results, one may conclude that the flowfield of the ogive nose cone will be dominated by centrifugal instability. One would also conclude that counterrotating vortices would be expected in the boundary layer of a more blunt (total angle $2\theta > 60$ deg) ogive nose cone in certain flow conditions.

From previous work, it is known that the same spiral vortices appear in the boundary layer of a 15-deg cone¹³ and in other types of spinning axisymmetric bodies.^{9,14,15}

For the purpose of detecting the decaying process of spiral vortices in more detail, a close-up picture was taken of an ogive nose cone (Fig. 4). One can observe the initially straight spiral vortices at the right of the picture. In the middle of the picture, the vortices are regularly arranged into horseshoe-like patterns along the axis of the spiral vortex. As one proceeds to the left, these horseshoe patterns break down into turbulence. In the case of cones, these horseshoe patterns also appear¹² with their vortices residing on the surface of the spiral vortices in a manner that is counterrotating with its neighbor. It seems that the horseshoe pattern observed on cones is the same as that on ogive nose cones, indicating a similar velocity field. A characteristic of these vortex disturbances is that they travel along the surface of the spiral vortices with a certain phase velocity relative to the wall and originate on the surface of the spiral vortices where very steep or near-discontinuous velocities are expected. This

Received June 6, 1984; revision received Oct. 10, 1984. Copyright © American Institute of Aeronautics and Astronautics, Inc., 1984. All rights reserved.

*Lecturer, Institute of High Speed Mechanics.

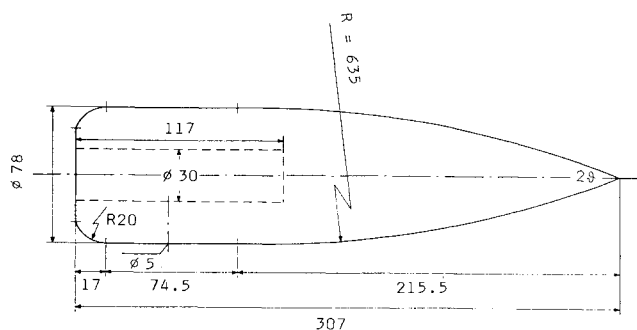
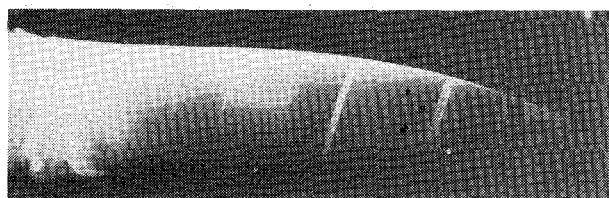
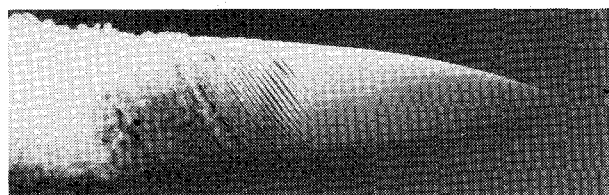


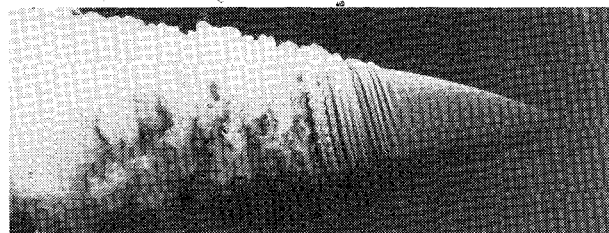
Fig. 1 Configuration of an experimental model.



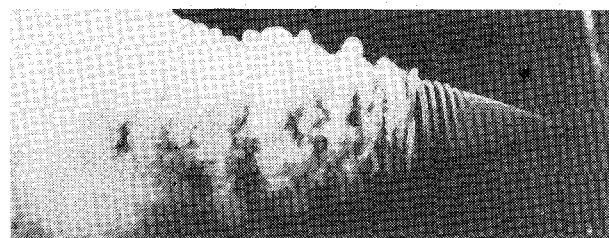
a) $N = 300$ rpm, $U_\infty = 4.8$ m/s.



b) $N = 1000$ rpm, $U_\infty = 3.4$ m/s.



c) $N = 1000$ rpm, $U_\infty = 1.2$ m/s.

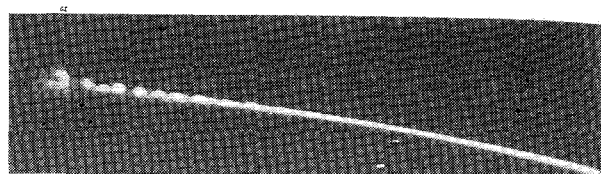


d) $N = 1000$ rpm, $U_\infty = 0.4$ m/s.

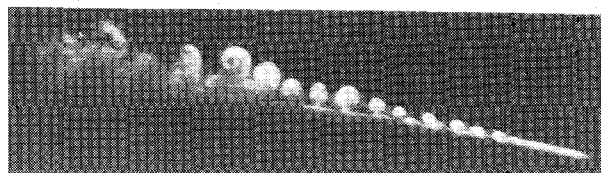
Fig. 2 Flow around an ogive nose cone.

would indicate that the horseshoe patterns are created by a viscous instability such as the Tollmien-Schlichting type. This same sort of experiment was performed by Mueller et al.⁶ In their research, they pointed out that Tollmien-Schlichting waves and cross-flow vortices (the spiral vortices of our case) can exist simultaneously for certain flow speed ratios with the secant-ogive nose cone model. However, in the case of our ogive nose cone, we were unable to detect such a condition.

Tollmien-Schlichting waves are strongly influenced by the spiral vortices' three-dimensional aspect and appear only in the last stage of the transition region of the spiral vortices. This same instability can also be found in Fig. 12 of Ref. 6. Because of this, the appearance of this instability and its



a) $N = 1000$ rpm, $U_\infty = 2.6$ m/s.



b) $N = 1000$ rpm, $U_\infty = 1.2$ m/s.

Fig. 3 Structure of the spiral vortices.

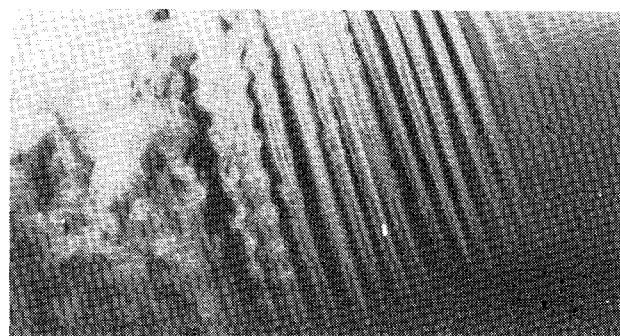


Fig. 4 Turbulent transition process of the spiral vortices ($N = 1000$ rpm, $U_\infty = 1.2$ m/s).

form is strongly influenced by such experimental conditions as the shape of the body, etc. Mueller's secant-ogive nose cone has two discontinuities in its surface curve. The most important of these is that where the cone attaches to the cylindrical body. This discontinuity may have induced an inflectional component in the velocity profile along the body and thus a Tollmien-Schlichting instability. This portion of the body is a region of instability in the spiral vortices induced by centrifugal force. Therefore, it could be said that the Tollmien-Schlichting instability is induced by three-dimensional spiral vortices in our case, while it is induced by the inflexional nature of the mean flowfield in Mueller's case.

Acknowledgment

Part of the work was performed during the author's stay at the Deutsche Forschungs und Versuchsanstalt für Luft- und Raumfahrt (DFVLR-AVA), Göttingen, FRG, which was sponsored by the Alexander von Humboldt Foundation. The author expresses his gratitude for this support. The author would also like to thank Dr. G. Allen for his kind assistance in proper English usage.

References

- ¹Morton, J. B., Jacobson, I. D., and Sanders, S., "Experimental Investigation of the Boundary Layer on a Rotating Cylinder," University of Virginia, Charlottesville, Rept. SS-3318-112-74, May 1974.
- ²Sturek, W. B., "Boundary Layer Studies on a Spinning Tangent-Ogive Cylinder Model," Ballistic Research Laboratories, Rept. 1801, July 1975.
- ³Okamoto, T., Yagita, M., and Kamijima, Y., "Experimental Investigation of the Boundary-Layer Flow over Rotating Cone-Cylinder Body in a Uniform Stream," *Bulletin of the Japan Society of Mechanical Engineers*, Vol. 19, 1976, pp. 930-937.

⁴Mueller, T. J., Nelson, R. C., Kegelman, J. T., and Morkovin, M. V., "Smoke Visualization of Boundary-Layer Transition on a Spinning Axisymmetric Body," AIAA Paper 81-4331, Dec. 1981.

⁵Kobayashi, R., Kohama, Y., and Kurosawa, M., "Boundary-Layer Transition on a Rotating Cone in Axial Flow," *Journal of Fluid Mechanics*, Vol. 127, 1983, pp. 341-352.

⁶Kegelman, J. T., Nelson, R. C., and Mueller, T. J., "The Boundary Layer on an Axisymmetric Body with and without Spin," *AIAA Journal*, Vol. 21, Nov. 1983, pp. 1485-1491.

⁷Kobayashi, R., Kohama, Y., and Takamade, Ch., "Spiral Vortices in Boundary Layer Transition Region on a Rotating Disk," *Acta Mechanica*, Vol. 35, 1980, pp. 71-82.

⁸Kohama, Y., Kobayashi, R., and Ito, H., "Performance of the Small Low-Turbulence Wind Tunnel, Tohoku University," *Memoirs of the Institute of High Speed Mechanics*, Tohoku University, Japan, Vol. 48, 1980, pp. 119-142.

⁹Kohama, Y. and Kobayashi, R., "Behaviour of Spiral Vortices on Rotating Axisymmetric Bodies," *Report of Institute of High Speed Mechanics*, Tohoku University, Japan, Vol. 47, 1983, pp. 27-38.

¹⁰Kohama, Y., "Study on Boundary Layer Transition of a Rotating Disk," *Acta Mechanica*, Vol. 50, 1984, pp. 193-199.

¹¹Gregory, N., Stuart, J. T., and Walker, W. S., "On the Stability of Three-Dimensional Boundary Layers with Application to the Flow Due to a Rotating Disk," *Philosophical Transactions of the Royal Society of London*, Ser. A, Vol. 248, 1955, pp. 155-199.

¹²Kohama, Y., "Behaviour of Spiral Vortices on a Rotating Cone in Axial Flow," *Acta Mechanica*, Vol. 51, 1984, pp. 105-117.

¹³Kobayashi, R. and Kohama, Y., "Vortices in Boundary Layer Transition on a Rotating Cone," *Proceedings of Second IUTAM Symposium on Laminar-Turbulent Transition*, Novosibirsk, USSR, July 1984.

¹⁴Kobayashi, R. and Izumi, H., "Boundary Layer Transition on a Rotating Cone in Still Fluid," *Journal of Fluid Mechanics*, Vol. 127, 1983, pp. 353-364.

¹⁵Kohama, Y. and Kobayashi, R., "Boundary Layer Transition and the Behaviour of Spiral Vortices on Rotating Spheres," *Journal of Fluid Mechanics*, Vol. 137, 1983, pp. 153-164.

Enhancement in Laser-Induced Impulse Imparted to a Surface in Supersonic Flow

Girard A. Simons

Physical Sciences Inc., Andover, Massachusetts

Introduction

IN a recent article, Woodroffe et al.¹ observed an increase in the laser-induced impulse imparted to a surface when in a supersonic flow. Impulse data, taken in 1 atm static air ($I_{no\ flow}$), were compared to those taken in a blowdown wind tunnel with 1 atm static pressure (I_{flow}). Their data indicate

$$I_{flow} \sim (1.2-2.0)I_{no\ flow}$$

Theoretical studies using the model of Reilly et al.² suggested that enhancement occurs as a result of an increase in gas density in the region of the flowfield where the laser energy is deposited. This increase in gas density is due to the lower gas temperatures occurring in a blowdown tunnel. The model suggests

$$I_{flow} \div 2I_{no\ flow}$$

which does not uniformly explain the data. Here, the momentum enhancement E is defined as

$$E = \frac{I_{flow}}{I_{no\ flow}} - 1 \quad (1)$$

and the mechanisms of enhancement are re-examined. It is concluded that the local gas density does not uniformly control the enhancement. There are several regimes in which the dynamic pressure of the gas and the local gas temperature will control momentum enhancement.

Flowfield Interactions

When a single, high-power laser pulse irradiates a surface, a laser-supported detonation wave (LSD) forms above the surface and propagates into the background gas. The high-pressure gas behind the LSD wave transfers momentum to the surface. This pressure p_s is expressed³ in terms of the laser intensity I_0 , gas density ρ , and the ratio of specific heats γ as

$$p_s = a_3 (I_0^2 \rho)^{1/2}$$

where $a_3 = 0.15$ for $\gamma = 1.2$

When a blunt object is placed in a highly supersonic flow, the gas pressure on the object is approximately the dynamic pressure of the gas ρu^2 , where u is the gas velocity. This pressure is approximately the total pressure of the gas behind a plane normal shock wave p_0 . If the pressure of the plasma p_s is much greater than p_0 , the plasma initially expands as though the background gas were static and the interaction of the expansion with the background gas becomes a late-time or far-field problem. However, when p_0 is of the same order as p_s , the plasma cannot expand and the interaction is termed a near-field problem.

Near-Field Interaction

In the near-field interaction, the plasma pressure p_s occurs over the spot radius (or laser beam radius) R_s . The plasma acts as a blunt body that experiences pressure p_0 acting over dimension R_s . Both p_s and p_0 decay together and hence act over the same time scale. Therefore, it follows that the impulse enhancement E is of the order of p_0/p_s . Thus,

$$E = \mathcal{O}(p_0/p_s) \quad (2)$$

where

$$p_0 = \rho u^2 \quad (3)$$

The data of Woodroffe¹ are compared to Eq. (2) in Fig. 1. The enhancement data decrease with increasing laser intensity, as predicted. The data may also be compared to the model predictions of Ref. 1 ($E = 1$ corresponding to $I_{flow} = 2I_{no\ flow}$). This suggests that it is the near-field interaction, not the effect of local gas density, that is responsible for the observed enhancement. The model and the data indicate that the near-field interaction is significant only when the induced pressure p_s is less than the dynamic gas pressure p_0 . Since the surface must be designed to withstand pressure p_0 , near-field enhancement is of no practical significance.

Far-Field Interaction

When the pressure due to the LSD wave is very much greater than the pressure on the surface ($p_s \gg p_0$), the early-time LSD wave and subsequent blast wave effectively propagate into a stationary atmosphere. Only the late-time blast wave, in the limit that the pressure behind the blast wave approaches p_0 , will experience the effect of the flow. Since the late-time blast wave has propagated to a location far from the irradiated spot, this is clearly a far-field interaction. To show this, an impulse model⁴ developed for stationary flow has been utilized. The effective stationary flow is taken to be the